Electrochemical Reduction of Azo Sulfonates and Sulfones. A Cyclic Voltammetry and EPR Study

Peter Rapta,[a] Andrej Staško,*[,a] Dušan Bustin,[b] Oskar Nuyken[c] and Brigitte Voit[c]
[a] *Department of Physical Chemistry, Slovak Technical University, CS-812 37 Bratislava, Czechoslovakia*
[b] *Department of Analytical Chemistry, Slovak Technical University, CS-812 37 Bratislava, Czechoslovakia*
[c] *Macromolecular Chemistry I, University of Bayreuth, 8580 Bayreuth, Germany*

Two reduction peaks can be seen in cyclic voltammograms of azo compounds such as $X-C_6H_4-N_2-Y$, where X is *o*-, *m*-, *p*-OCH_3, *m*-, *p*-CH_3, *p*-Cl, *p*-NO_2, di-*o*-CO_2CH_3, di-*o*-CO_2H and Y is $-SO_3Na$, $-SO_2Ph$, $-BF_4$, $-CCH_3(CN)_2$, $C(CH_3)_2CN$, investigated in acetonitrile. Their degree of reversibility depends on the substituents X and Y. Sulfonates and sulfones form anion radicals in the first reduction wave, as detected by electron paramagnetic resonance (EPR) spectroscopy, with unpaired spin density centred on the azo nitrogens and distributed also over the phenyl ring. The reduction products of azo compounds decompose with elimination of N_2 and the radicals thus formed terminate either by abstracting hydrogen from the solvent and the supporting electrolyte, or by forming cage products.

Azo compounds are well known and widely used in chemistry and pharmacy, and have been the subject of numerous electrochemical[1,2] and EPR investigations.[3,4] Increasingly numerous applications of sulfur-containing azo compounds in polymer chemistry[5] and photo resin processes[6] focused our attention on the question of their electrochemical activation, on the path of their decomposition, and on the radical products formed in their reactions. In the present paper we report on some cyclic voltammetric and EPR studies of azo sulfonates and azo sulfones and some related azo compounds in aprotic solvents, mainly acetonitrile. The characteristics of the cyclic voltammograms are presented. The analysed EPR spectra of the anion radicals of the azo compounds and their consecutive products formed during cathodic reduction are described, and the structure of the observed radical products is suggested.

Experimental

The azo compounds **1a–e**, **2a–e**, **3** and **4a,b** were investigated.

The preparation of **1a–d**, **2** and **4** is described in refs. 7 and 8; the preparation of **1e**, **f** is described in ref. 9; while **3**, spin traps nitroso-*tert*-butane (NtB; 2-methyl-2-nitrosopropane) and nitrosodurene (ND) were commercial products from Aldrich.

The solvents employed, acetonitrile (AN), dimethylform-

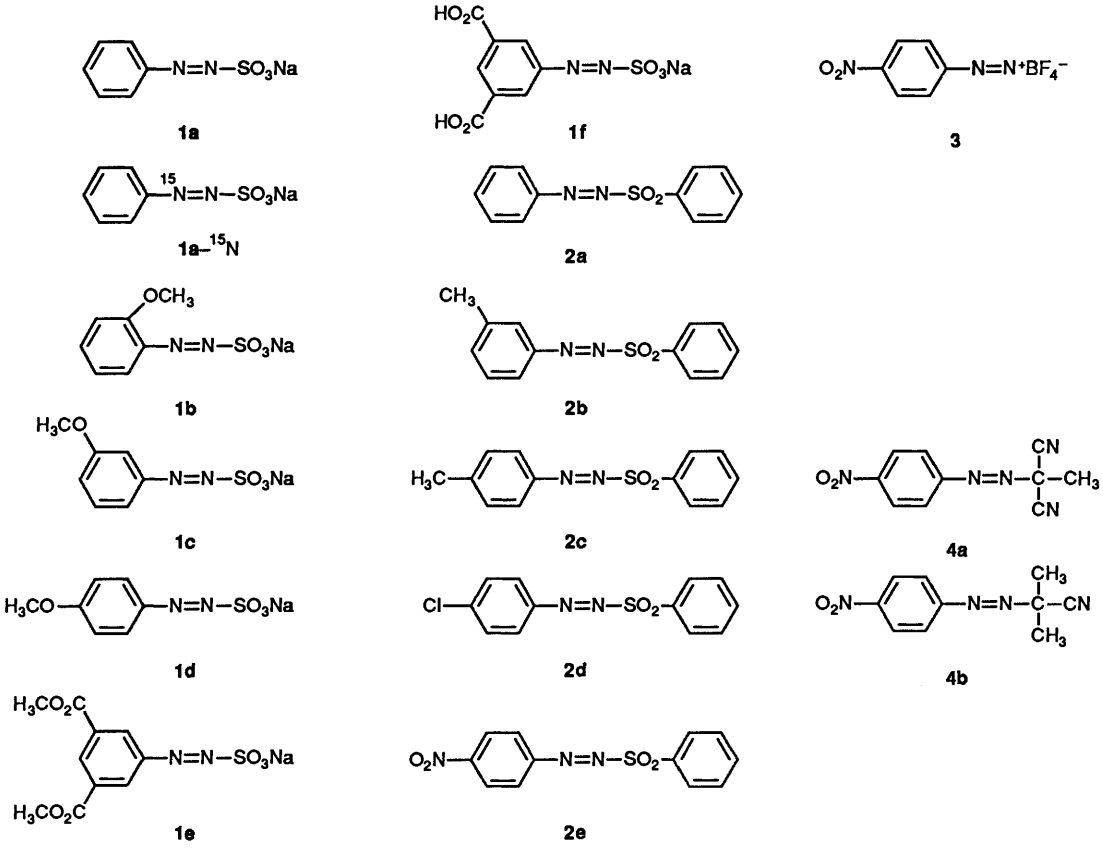

Table 1 Voltammetric data[a] of azo compounds **1** and **2** found by cathodic reduction in AN [1 × 10^{-3} mol dm^{-3}, 0.1 mol dm^{-3} TBAP, Pt electrode, SCE reference]

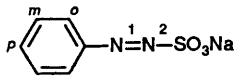

1[b]

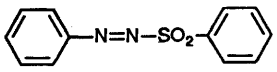

2[c]

Structure	X	E^1_{pc}	E^2_{pa}	ΔE^1_p	E^2_{pc}
1a	H	1.12	0.86	0.32	1.5
1b	*o*-OCH_3	1.15	0.83	0.32	1.5
1c	*m*-OCH_3	1.15	0.85	0.30	1.5
1d	*p*-OCH_3	1.22	0.87	0.35	1.5
1e	*m,m*-CO_2CH_3	1.11	0.76	0.35	1.5
1f	*m,m*-CO_2H		not observed		
2a	H	0.82	0.61	0.21	1.00
2b	*m*-CH_3	0.84	0.69	0.15	1.80
2c	*p*-CH_3	0.80	0.65	0.15	1.86
2d	*p*-Cl	0.72	0.57	0.15	1.72
2e	*p*-NO_2	0.45	0.32	0.13	0.77

[a] E^1_{pc}, cathodic peak potentials; E^1_{pa}, anodic peak potential; $\Delta E^1_p = E^1_{pc} - E^1_{pa}$ (first reduction wave); E^2_{pc}, cathodic peak potential (second reduction wave). [b] Scan rate = 100 mV s^{-1}. [c] 167 mV s^{-1}.

amide (DMF), and methylene dichloride (MDC) of analytical purity, were first dried over molecular sieves and later over P_2O_5, and vacuum distilled. The electrochemical reduction was mainly carried out in AN containing 10^{-3} mol dm^{-3} of substrate and 10^{-1} mol dm^{-3} of tetrabutylammonium perchlorate (TBAP) under an argon atmosphere. The cyclic voltammetric experiments were performed with the multipurpose polarograph GWP 673 (Academy of Sciences, Germany) and the XY-recorder ENDIM, 620.02 (Germany) employing a three-electrode system involving a platinum working electrode, a platinum auxiliary electrode and a reference saturated calomel electrode (SCE) equipped with a Luggin capillary. The ferrocenium/ferrocene internal potential marker[10] was used to compare redox potentials in AN. *In situ* electrochemical EPR experiments were carried out in a Varian flat cell on a Bruker 200D spectrometer on line with an Aspect 2000 computer. The low temperature measurements were performed in a self-constructed cell.[11] EPR spectra were simulated employing a Bruker standard programme.

Results and Discussion

Electrochemical Studies.—Sulfones. The electrochemical properties of sulfones **2a–d** are similar. The typical cyclic voltammetric behaviour of this group is represented by compound **2d** in Fig. 1(*b*). Two reduction peaks at negative potentials can be observed on voltammograms of all of them. Their peak potentials E_{pc} and some further voltammetric data are given in Table 1. The first cathodic peak exhibits a corresponding anodic peak upon scan reversal. Their potential difference is about 120 mV. The second electron transfer step gives no corresponding anodic peak. The ratio of anodic (i^1_{pa}) to cathodic (i^1_{pc}) peak currents for the first step is close to unity (evaluated according to Bontempelli's equation).[12] The first electrochemical step produces a stable anion radical indicated by EPR spectroscopy as described below. The second irreversible step leads to the formation of a dianion, the lifetime of which is sufficiently short to preclude a cyclic voltammetric anodic peak for its reoxidation. Rapid reaction of the dianion probably involves its protonation, as dianions react rapidly with proton donors.[1] A slightly different behaviour as compared with this group was shown by the *para*-nitro

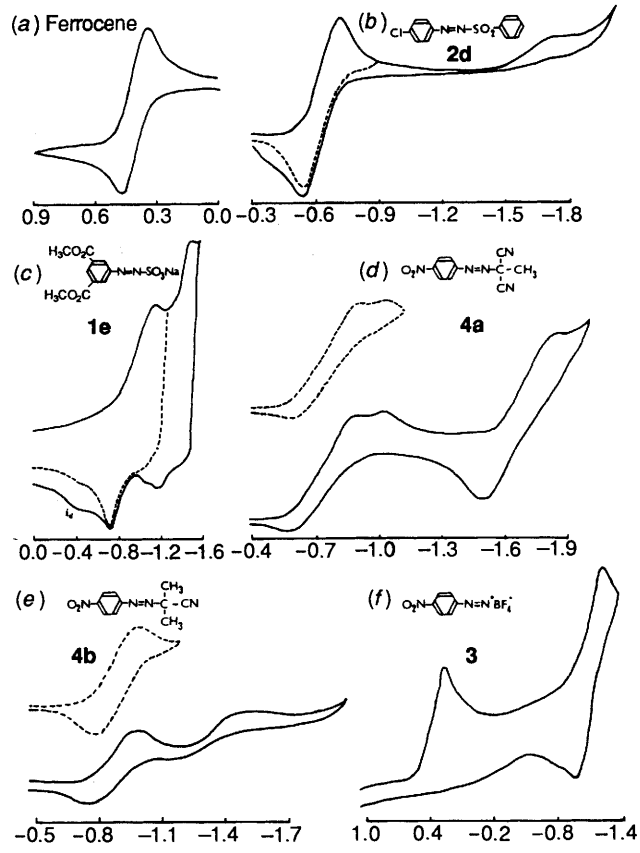

Fig. 1 Cyclic voltammograms of (*a*) ferrocene and azo compounds (*b*) **2d**, (*c*) **1e**, (*d*) **4a**, (*e*) **4b** and (*f*) **3** obtained in acetonitrile. Potentials are referred to SCE.

substituted azo sulfone **2e**, the second step of which has been found to be reversible. This is evidently due to an additional possibility for the delocalization of the negative charge on the nitro group in **2e**, accompanied by increased stability of the dianion formed.

Sulfonates. The cyclic voltammetric behaviour of sulfonates is distinctly different from that of sulfones. A typical voltammogram of this group is represented by compound **1c** in Fig. 1(*c*). The separation of the anodic (E^1_{pa}) and of the cathodic (E^1_{pc}) peak potentials is about 300 mV (see Table 2). This implies a quasi-reversible process on the platinum electrode. In the simultaneous electrochemical–EPR experiments (SEEPR) the corresponding anion radicals were observed. The potential of the second wave (E^2_{pc}) here is closer to the first one compared to sulfones. This can be explained by a weaker acceptor effect of the sulfonate group $-SO_3^-$. Additionally a second effect is probably involved, namely the disproportionation of the monoanion in the presence of sodium ions, and stabilization of the dianion by the formation of ion pairs with Na^+. Similar observations were also reported in ref. 1, where, on the addition of Li^+ or other ions, the first and second reduction wave of azo compounds moved closer together until a single two-electron transfer occurred. Consequently, the current i_d [Fig. 1(*e*)] is ascribed to the reoxidation of species consisting of azo dianions and Na^+ or $(C_4H_7)_4N^+$ cations. Such species are formed as a result of a dismutation reaction; therefore, the current i_d may be observed on CV curves, even if the electrode is polarised to the potentials of the first wave only.[13]

Other azo compounds. One of the most discussed problems of the activated azo compounds is the path of their decomposition, which can be either synchronous ($R-N_2R \longrightarrow$

Table 2 Assignment of splitting constants obtained by simulation of EPR spectra of anion radicals cathodically generated in acetonitrile from compounds **1a–f** and **2a–e**

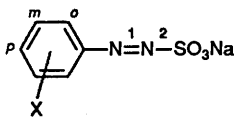

1

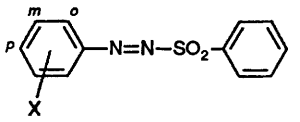

2

Compound	X	Splitting constants/mT a_N^1	a_N^2	a_H^o	a_H^m	a_H^p	a_X	*g* Values
1a	H	0.5892	0.618	0.248 0.3505	0.0735 0.107	0.378	—	2.0040
1a-^{15}N		0.8320	0.6185	0.248 0.3505	0.0735 0.107	0.378	—	2.0040
1b	*o*-OCH_3	0.58 (0.5885)	0.5885 (0.58)	0.3931	0.0535 0.1135	0.3931	—	2.0040
1c	*m*-OCH_3	0.59 (0.6)	0.6 (0.59)	0.252 0.3325	0.074	0.389	—	2.0040
1d	*p*-OCH_3	0.5762 (0.641)	0.641 (0.5762)	0.2547 0.3815	0.098 0.098		0.0293 (3 H)	2.0040
1e	*m,m*-CO_2CH_3	0.47	0.636	0.184		0.442	—	2.0039
1f	*m,m*-CO_2H	0.58 (0.686)	0.686 (0.58)	0.2515		0.375	—	2.0041
2a	H	0.8691	0.362	0.33	0.1196	0.4065	—	2.0041
2b	*m*-CH_3	0.8685	0.334	0.334 0.378	0.116	0.4065	0.116 (3 H)	2.0041
2c	*p*-CH_3	0.8648	0.3751	0.369 0.369	0.123 0.123		0.4348 (3 H)	2.0041
2d	*p*-Cl	0.832	0.3805	0.3225 0.3825	0.126 0.126		0.019 (Cl)	2.0044
2e	*p*-NO_2	0.556	0.455	0.239 0.3	0.09 0.09		0.032 (N)	2.0043

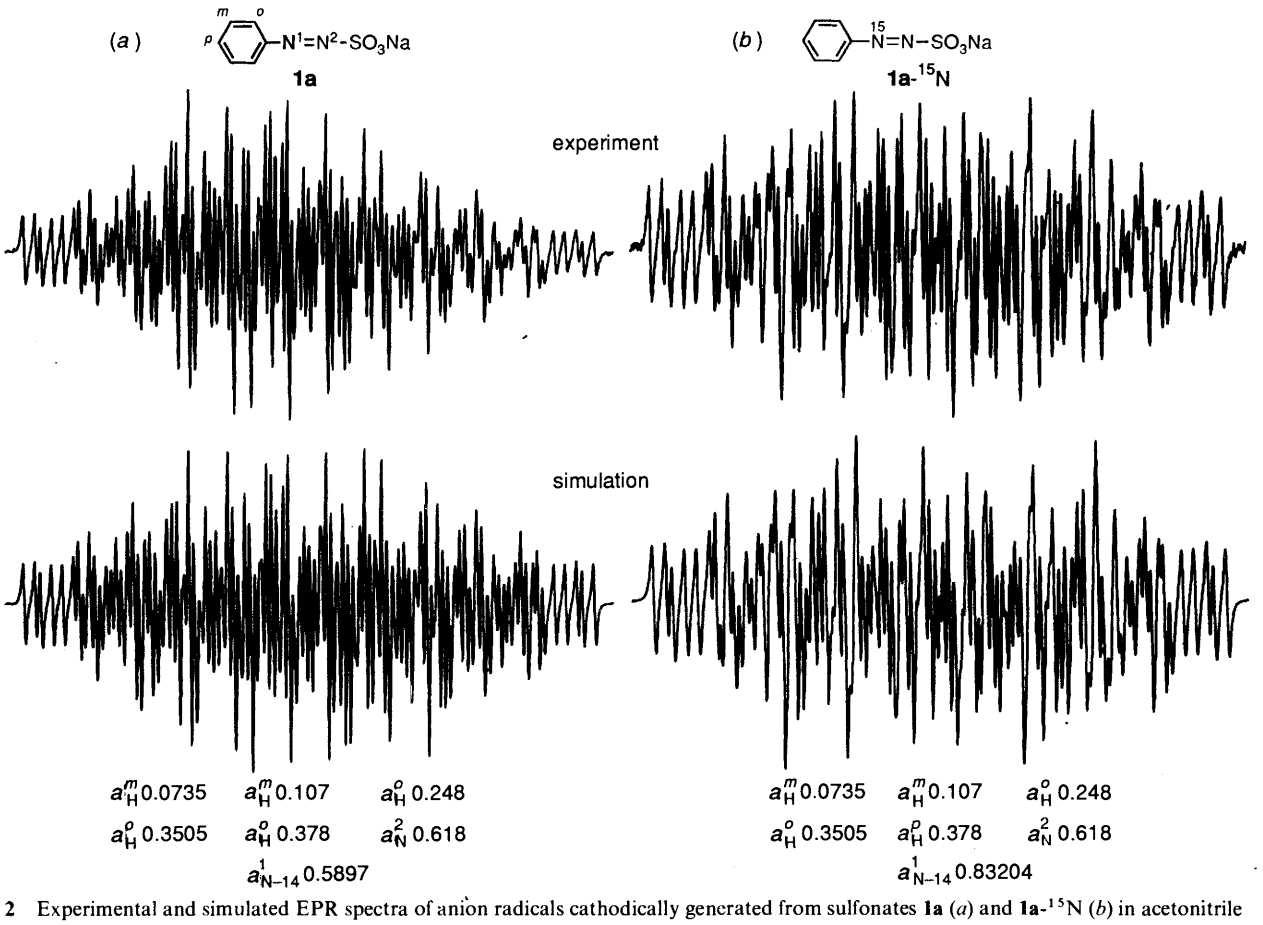

Fig. 2 Experimental and simulated EPR spectra of anion radicals cathodically generated from sulfonates **1a** (*a*) and **1a**-^{15}N (*b*) in acetonitrile

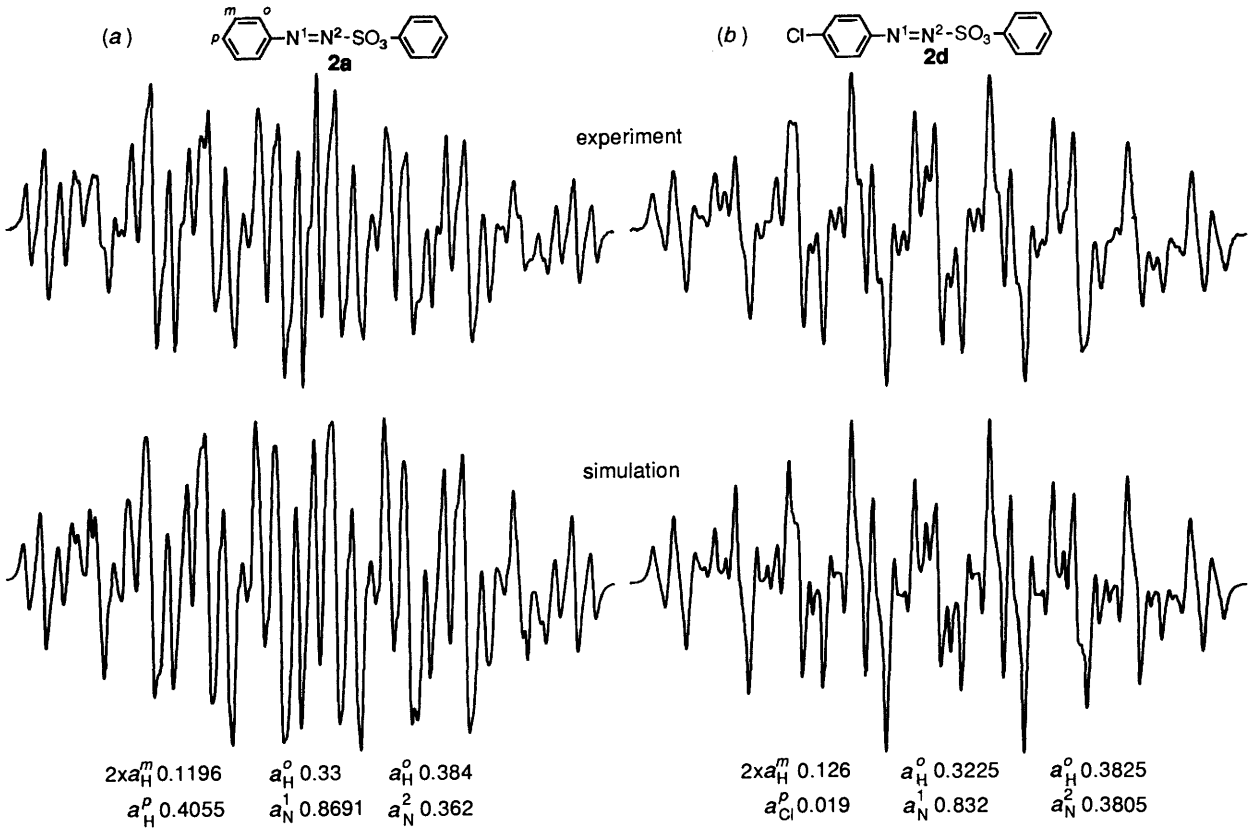

Fig. 3 Experimental and simulated EPR spectra of anion radicals cathodically generated from sulfonates **2a** (*a*) and **2d** (*b*) in acetonitrile

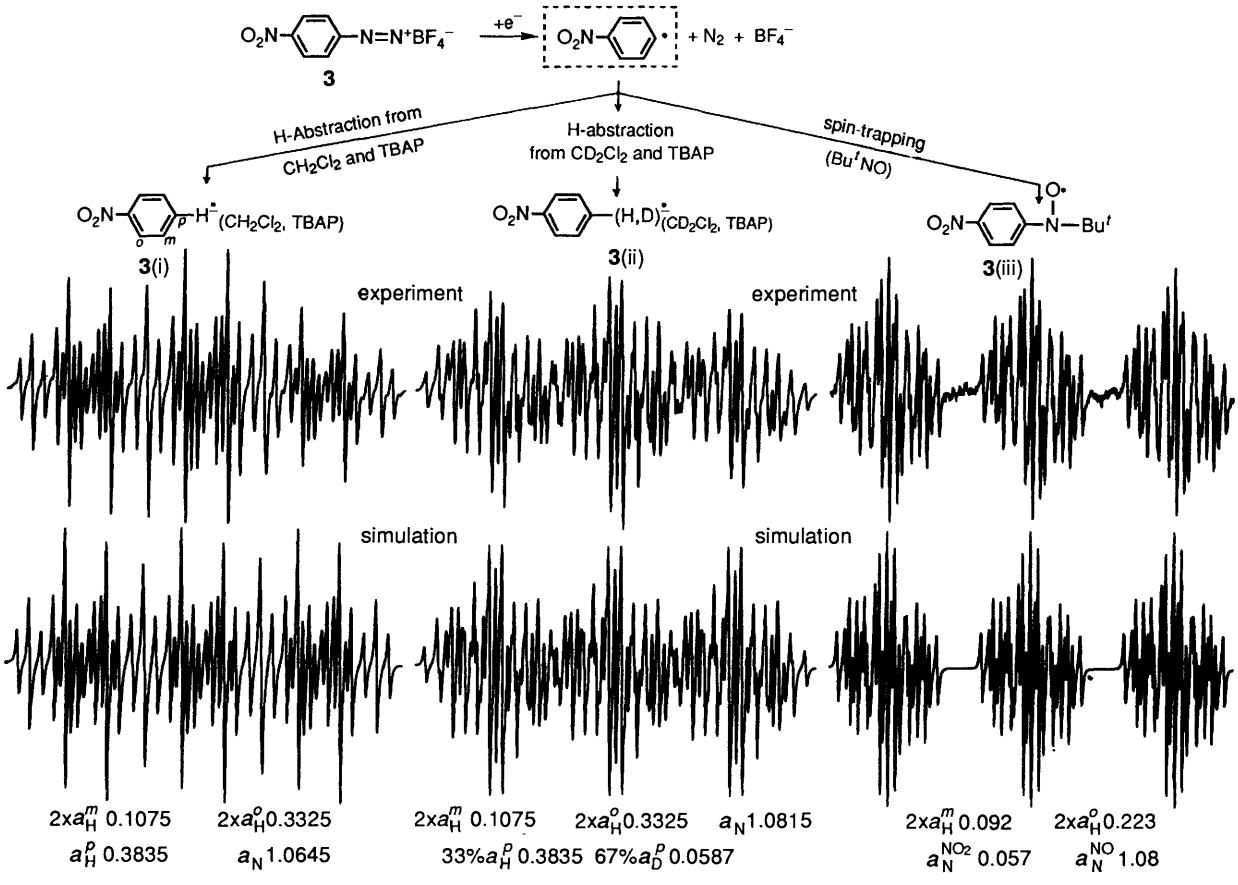

Fig. 4 Experimental and simulated EPR spectra found in the cathodic reduction of azo compound **3** and assigned to the following products: **3**(i) *p*-nitrobenzene anion radical, **3**(ii) nitrobenzene anion radicals with 33% hydrogen and 67% deuterium in the *para* position and **3**(iii) spin adduct of *p*-NO_2–C_6–$H_4^{\bullet}$ radical to Bu^{t}NO

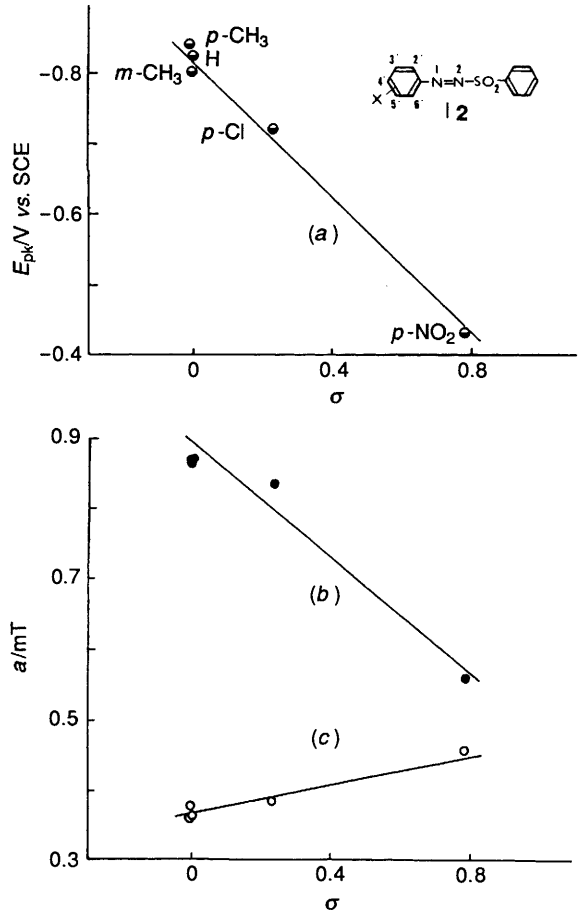

Fig. 5 The dependence of cathodic peak potentials (*a*), nitrogen splitting constants a_N^2 (b) and a_N^1 (*c*) on the Hammett constants of anion radicals generated from variously substituted sulfones **2a–e**.

$R^{\bullet} + N_2 + R^{\bullet}$) or asynchronous ($R{-}N_2R \longrightarrow R{-}N_2^{\bullet} + R^{\bullet}$). To obtain some additional information on this problem, a few further azo compounds, *e.g.* **3** and **4a**, **b** were investigated. By a one-electron reduction of **3** one should expect to observe directly the product of an asynchronous decomposition ($RN_2^+ + e^- \longrightarrow RN_2^{\bullet}$). The cyclic voltammetric investigations of the first reduction wave of **3** have shown a high degree of irreversibility, which points to very limited stability of the $RN_2^{\bullet}$ radical. By SEEPR measurements, no $RN_2^{\bullet}$ radical was detected but its decomposition products were found as described below. The second wave is nearly reversible ($\Delta E_p = 160$, i_{pa}/i_{pb} *ca.* 1), without further additional radical products. CV curves of compounds **4a** and **4b** are presented in Fig. 1(*d*), (*e*). In the case of compound **4a**, the first wave is totally irreversible; the second one is quasi-reversible. On the other hand in the case of compound **4b**, the first wave exhibits a quasi-reversible character, but the second step is irreversible. Neither compound **4a** nor **4b** forms the radical $RN_2^{\bullet}$, but they do form other radical products discussed later.

SEEPR Measurements.—Sulfonates. In Fig. 2 are shown two selected experimental and simulated EPR spectra of anion radicals generated from unsubstituted basic sulfonate **1a** and from its ^{15}N-labelled analogue **1a**-^{15}N. They were generated at the potential of the first reduction wave. The splitting constants obtained by simulating the spectra of all investigated sulfonates **1a–f** are summarized in Table 2. Their assignment is based upon the following arguments. From the two approximately equal nitrogen splitting constants for the structure **1a**, the lower one (a_N^1) was assigned to the nitrogen attached to the phenyl group on the basis of the experiment with ^{15}N-labelled nitrogen in position N(1), where the spectrum **1a**-N^{15} shown in Fig. 2 was observed. It was simulated by exchanging only the parameter of a_{14-N}^1 in **1a** with the corresponding parameter of a_{15-N}^1 in **1a**-^{15}N (Fig. 2, Table 2). Analogously, in the remaining structures **1c–f**, we suggest the assignment of the lower splitting constant to the N(1) nitrogen. But, owing to the negligible differences between the a_N^1 and a_N^2 splitting constants, their reverse assignment in some cases cannot be excluded. Therefore, in Table 2 we also put in brackets another alternative *i.e.* the reverse assignment of a_N^1 and a_N^2. Especially interesting here is the fact that the values of the splitting constants thus assigned to a_N^1 and a_N^2 in structures **1a–e** correlate with the Hammett constants of the substituents; the slope for a_N^1 is negative $\rho = -0.05$, (with correlation coefficient $r = 0.52$), while for a_N^2 it is positive $\rho = 0.05$, ($r = 0.69$). The remaining hyperfine splittings in the structures given in **1** can originate only from hydrogens on the phenyl ring. According to their values, they can be divided into two groups: (i) three protons with the higher values (0.25–0.45 mT) and (ii) two protons with lower values (0.07–0.12 mT). Evidently, in agreement with the generally known distribution of unpaired electrons on an aromatic ring, the splittings with the higher values, group (i), can be assigned to the *ortho* and the *para* protons and those with the lower ones, group (ii), to the *meta* protons. This was confirmed by our further experiments, since upon replacing the *ortho* (structure **1b**) or *para* hydrogen (structure **1d**) with the methoxy group, one splitting constant with a higher value was eliminated. Additionally, upon replacing the *meta* hydrogen with 3′-OCH_3, 3′,5′-CO_2CH_3 and 3′,5′-CO_2H, the splitting constants with lower values were eliminated. The highest value of splitting constants in group (i) was assigned to the *para* proton, and the two lower values to the *ortho* protons.

Sulfones. Two selected EPR spectra measured by the cathodic reduction of sulfones **2b** and **2e** at the first wave are shown in Fig. 3. The splitting constants obtained by the simulation of the spectra of all investigated sulfones are summarized in Table 2. There is a striking difference between the above described sulfonates (with nearly equal nitrogen splitting constants a_N^1 and a_N^2; their mean difference is only *ca.* 0.1 mT) and sulfones (the difference is *ca.* 0.5 mT). This is due to the stronger acceptor properties of $-SO_2Ph$ as compared with the $-SO_3^-$ group. The $-SO_2Ph$ group causes a lowering of spin density on the neighbouring atom, *i.e.* the N(2) nitrogen, more than the $-SO_3^-$ group, and therefore we assigned the lower splitting constants (*ca.* 0.35 mT) to the nitrogen in position 2 and the higher ones (*ca.* 0.85 mT) to position 1 as given in Table 2. The sulfones and the sulfonates are similar in that the assigned nitrogen splitting constants a_N^1 and a_N^2 correlate well with Hammett constants. They show again a negative sign of the slope with $\rho = -0.37$ mT, ($r = -0.96$) for a_N^1 and positive $\rho = 0.12$ mT, ($r = 0.92$) for a_N^2 as depicted in Fig. 5.

The assignment of the hydrogen splittings here is straightforward. The highest splitting constant (*ca.* 0.4 mT) was assigned to the *para* proton, the next two highest constants (*ca.* 0.35 mT) to the *ortho* and the two lowest ones (*ca.* 0.15 mT) to the *meta* protons. Also in accord with such an assignment are the splitting constants found for the *para*-methyl substituted phenyl group in **2c** with $a_H^4(CH_3) = 0.444$ mT and for chlorine in **2d** with $a_{Cl}^p = 0.019$ mT. The splitting constant for *para*-methyl protons in **2c** (0.444 mT), if compared to that of the proton in unsubstituted **2a** (0.405 mT), suggests the π-character of the corresponding radical. Nearly equivalent *ortho* protons imply rather free rotation of that phenyl group in the sulfones, which is not the case for the sulfonates.

Other azo compounds and their radical products. In accord with the observed high degree of irreversibility of the first reduction wave of compound **3**, the radical $RN_2^{\bullet}$ was not

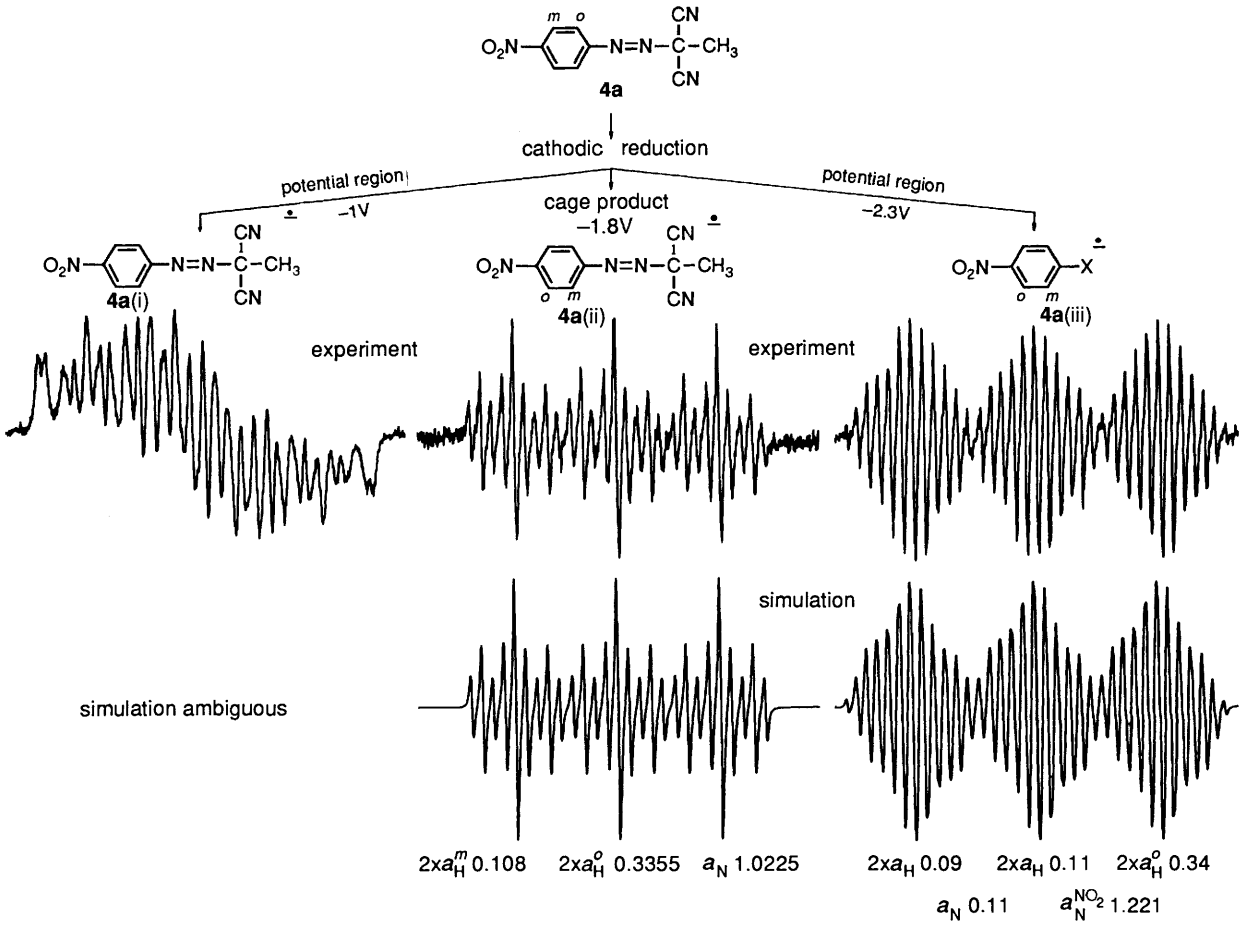

Fig. 6 Experimental and simulated EPR spectra obtained at various potentials in the cathodic reduction of azo compound **4a**, and their assignment to the following radicals: **4a**(i), anion radical of **4a**; **4a**(ii), anion radical of a direct cage product after N_2-elimination and **4a**(iii) anion radical of a modified cage product

found by SEEPR measurements, but spectrum **3**(i) given in Fig. 4 was observed. Its simulation is comparable with the already known[14] nitrobenzene anion radical. Consequently the formation of the *p*-nitrophenyl radical intermediates in the decomposition of $RN_2^{\bullet}$ ($RN_2^{\bullet} \longrightarrow R^{\bullet} + N_2$) has to be assumed. Next the *para* position abstracts a hydrogen from the support electrolyte and so forms a nitrobenzene anion radical. We verified this in an experiment using deuteriated dichloromethane CD_2Cl_2 where spectrum **3**(ii) shown in Fig. 4, was observed. It was simulated as the sum of two different spectra of *p*-nitrobenzene anion radical; the first one (67%) with deuterium in the *para* position (abstracted from CD_2Cl_2) and the second one (33%) with hydrogen in the *para* position (abstracted from TBAP). The simulated sum of these spectra **3**(ii) in Fig. 4 is in good agreement with the experiment. It is noteworthy that the splitting constant $a_N = 1.0645$ mT [spectrum **3**(i)] of the nitrobenzene anion radical in CH_2Cl_2 increased to $a_N = 1.0815$ mT [spectrum **3**(ii)] in the experiment with deuteriated CD_2Cl_2. In order to prove the formation of *p*-nitrophenyl intermediates, NtB and ND were used as spin traps. The spectrum thus observed, **3**(iii), employing NtB, is given in Fig. 4 and confirms the formation of the phenyl trap product. Further spin trap experiments showed that it was not possible to observe the presumed $RN_2^{\bullet}$ radical even if the temperature was lowered to 200 K (in CH_2Cl_2).

Upon their photochemical and thermal activation azo compounds of type **4** form consecutive products where an azo group is evidently involved.[15] Therefore we followed the formation of radicals in their cathodic reduction. In the case of compound **4a**, at the first reduction wave (*ca.* 1 V) an anion radical **4a**(i) with $g = 2.0052$ was found. The simulation of the obtained spectrum was ambiguous, but its g value, its spectral width, and a few splitting constants extracted from a partial analysis, agree well with anion radicals of azo compounds. At higher potential (*ca.* 1.8 V) and current densities the anion racical **4a**(ii) shown in Fig. 6 was found. Its spectral parameters are compatible with the formation of the so-called cage product (O_2N–C_6–H_4–N_2–R + $e^- \longrightarrow O_2N$–C_6H_4–$R^{\bullet -}$ + N_2). At still higher potentials (*ca.* 2.3 V) and current densities a new radical product was found [spectrum **4a**(iii) in Fig. 6]. From its simulation a *para*-substituted nitrobenzene anion radical is evident with $a_N(NO_2) = 1.221$ mT, $a_H(ortho) = 0.34$ mT and $a_H(meta) = 0.11$ mT or 0.09 mT. Additionally, in its *para* position there is a group X with two hydrogen nuclei having splitting constants $a_H = 0.09$ mT or 0.11 mT, and one nitrogen nucleus with $a = 0.11$ mT. A partial structure like X ($-NH_2$) or X ($-N{=}CH_2$) would be compatible with the splitting constants obtained. No well-defined radical product was observable at the first irreversible wave of **4b**. At higher potentials only nitrobenzene anion radical was found.

In general, the formation of cage products in our experiments was usually observable at higher potentials and current densities, mainly in the region of the second reduction wave. In the case of compound **2a** at higher potential a cage product [similar to **4a**(ii)] was found with splitting constants $2 \times a_H^m = 0.0742$ mT, $2 \times a_H^o = 0.3086$ mT, $a_N = 1.3906$ mT.

Acknowledgements

We thank Slovak grant agency project A-114 and *Sonderforschungsbereich* of University of Bayreuth for support of this work.

References

1 J. P. Stradins and V. T. Glezer, in *The Encyclopedia of Electrochemistry of the Elements, Organic Section*, eds. A. J. Bard and H. Lund, Marcel Dekker, New York, 1979, vol. XIII, ch. XII-4, p. 163.
2 J. L. Salder and A. J. Bard, *J. Am. Chem. Soc.*, 1968, **90**, 1974.
3 F. A. Neugebauer and H. Weger, *Chem. Ber.*, 1975, **108**, 2703.
4 (*a*) E. T. Strom, G. A. Russell and R. Konaka, *J. Chem. Phys.*, 1965, **42**, 2033; (*b*) Ch. S. Johnson and R. Chang, *J. Chem. Phys.*, 1966, **43**, 3183; (*c*) G. A. Russell, R. Konaka, E. T. Strom, W. C. Danen, Kou-Yuan Chang and G. Kaup, *J. Am. Chem. Soc.*, 1968, **90**, 4646; (*d*) A. G. Evans, J. C. Evans, P. J. Emes, C. L. James and P. J. Pomery, *J. Chem. Soc. B*, 1971, 1484.
5 O. Nuyken and R. Weidner, *Adv. Polym. Sci.*, 1986, **73/74**, 145.
6 O. Nuyken and B. Voit, *Makromol. Chem.*, 1989, **190**, 132.
7 O. Nuyken, T. Knepper and B. Voit, *Makromol. Chem.*, 1989, **190**, 1325.
8 R. Kerber and O. Nuyken, *Makromol. Chem.*, 1973, **164**, 183.
9 J. Dauth, Ph.D. Thesis, University of Bayreuth, 1992.
10 S. K. Mandal, L. K. Thompson, M. J. Newlands and J. Gabe, *Inorg. Chem.*, 1989, **28**, 3707.
11 (*a*) P. Rapta, Ph.D. Thesis, Slovak Technical University, 1992; (*b*) R. Klusák, Ph.D. Thesis, Masaryk University, 1992.
12 G. Bontempelli, F. Magno and S. Daniele, *Anal. Chem.*, 1985, **57**, 1503.
13 H. Kryszczynska and M. Kalinowski, *Roczniki Chemii*, 1974, **48**, 1791.
14 A. Berndt, M. T. Jones, M. Lehnig, L. Lunazzi, G. Placucci, H. B. Stegmann and K. B. Ulmschneider, in *Landolt-Börnstein*, eds. H. Fisher and K.-H. Hellwege, Springer-Verlag Berlin, Heidelberg, New York, 1980, Group II, volume 9, part d 1, *Organic Anion Radicals*.
15 R. Kerber, O. Nuyken and V. Pasupathy, *Makromol. Chem.*, 1973, **170**, 155.

Paper 2/02589B
Received 19*th May* 1992
Accepted 10*th August* 1992